Signal Processing 137 (2017) 44–51

Contents lists available at ScienceDirect

Signal Processing

journal homepage: www.elsevier.com/locate/sigpro

Short communication

Reweighted smoothed l_0-norm based DOA estimation for MIMO radar

Jing Liu[a,b,*], Weidong Zhou[a], Filbert H. Juwono[b,c], Defeng (David) Huang[b]

[a] College of Automation, Harbin Engineering University, Harbin 150001, China
[b] School of Electrical, Electronic and Computer Engineering, The University of Western Australia, Australia
[c] Department of Electrical Engineering, Universitas Indonesia, Depok, Indonesia

ARTICLE INFO

Article history:
Received 21 November 2016
Revised 24 January 2017
Accepted 30 January 2017
Available online 31 January 2017

Keywords:
Multiple-input multiple-output radar
Direction of arrival estimation
Reweighted smoothed l_0-norm
Sparse representation

ABSTRACT

In this paper, a reweighted smoothed l_0-norm algorithm is proposed for direction-of-arrival (DOA) estimation in monostatic multiple-input multiple-output (MIMO) radar. The proposed method firstly performs the vectorization operation on the covariance matrix, which is calculated from the latest received data matrix obtained by a reduced dimensional transformation. Then a weighted matrix is introduced to transform the covariance estimation errors into a Gaussian white vector, and the proposed method further constructs the other reweighted vector to enhance sparse solution. Finally, a reweighted smoothed l_0-norm minimization framework with a reweighted continuous function is designed, based on which the sparse solution is obtained by using a decreasing parameter sequence and the steepest ascent algorithm. Consequently, DOA estimation is accomplished by searching the spectrum of the solution. Compared with the conventional l_1-norm minimization based methods, the proposed reweighted smoothed l_0-norm algorithm significantly reduces the computation time of DOA estimation. The proposed method is about two orders of magnitude faster than the l_1-SVD, reweighted l_1-SVD and RV l_1-SRACV algorithms. Meanwhile, it provides higher spatial angular resolution and better angle estimation performance. Simulation results are used to verify the effectiveness and advantages of the proposed method.

1. Introduction

With mutually orthogonal transmitted waveforms, multiple-input multiple-output (MIMO) radar has drawn increasing attention because of its advantages over conventional phased-array radar [1–3]. MIMO radar is generally grouped into colocated MIMO radar with enlarged virtual array aperture [2] and statistical MIMO radar. Furthermore, colocated MIMO radar is divided into bistatic MIMO radar and monostatic MIMO radar. For a certain target, the direction-of-departure (DOD) of the transmitted signal and the direction-of-arrival (DOA) of the echo are the same [2,3] in monostatic MIMO radar due to its closely-located arrays. Angle estimation is one of the most important research subjects in the fields of array signal processing and radar applications. In this paper, we focus on the angle estimation problem in monostatic MIMO radar.

A large number of subspace-based DOA estimation algorithms have been proposed [4–8], including MUSIC [6], reduced-dimension (RD) ESPRIT [7] and RD-Capon [8] methods for MIMO radar. On the other hand, the emerging application of sparse representation (SR) theory to angle estimation is a major breakthrough. This is because SR-based DOA estimation algorithms can achieve higher angle resolution than alternative methods, and they have the better ability to adapt to the challenging circumstances such as less snapshots [9]. In the sparse representation framework, the most ideal constraint for obtaining the sparse solution is the l_0-norm minimization. However, it is NP-hard. To solve this problem, different categories of sparse signal reconstruction methods [10–15], such as the classical l_1-norm minimization methods based on basis pursuit (BP) optimization principle [10], the matching pursuit (MP) [11], the focal underdetermined system solution (FOCUSS) [12] and the sparse Bayesian learning (SBL) [13] algorithms, have been proposed. MP and FOCUSS methods have less calculation burden than the BP algorithm, however, they provide worse signal reconstruction performance. On the other hand, although SBL method has the better ability to recover the signal, it requires much higher computational complexity than BP, MP and FOCUSS algorithms. Aiming at DOA estimation, it has been verified that the relaxed minimization based on l_1-norm, can guarantee the solution accuracy with reasonable computation time [9,16]. As a result, l_1-norm minimization is commonly used in SR-based DOA estimation algorithms [9,16–20], such as l_1-SVD (singular value decomposition) algorithm [9] and l_1-SRACV (sparse representation array covariance vectors) algorithm [17].

* Corresponding author.
E-mail address: liujing@hrbeu.edu.cn (J. Liu).

http://dx.doi.org/10.1016/j.sigpro.2017.01.034
0165-1684/

To improve the performance of the DOA estimation, some extended sparse representation methods have been proposed. In [18], by constructing a weight matrix with the coefficients of the RD-Capon spectrum, a reweighted l_1-SVD algorithm enhances the l_1-norm based sparse solution. Besides, the noncircular source-based sparse DOA estimation method enlarges the virtual array aperture by the use of the signal noncircularity [3]. However, it incurs much more calculation burden. On the other hand, for reducing the computational complexity of sparse signal recovery procedure, a real-valued (RV) l_1-SVD method [19] and a revised real-valued sparse DOA estimation algorithm [20] utilize the unitary transformation to avoid the complex-valued processing. In [19], RV l_1-SVD concerns the received data matrix and the singular value decomposition, and it involves the multiple measurement vector (MMV) problem. However, the method in [20] is based on the array covariance vector (ACV), and it involves the single measurement vector (SMV) problem. Thus, it has lower complexity than the RV l_1-SVD algorithm in [19]. For short, we call the method in [20] RV l_1-SRACV.

Although some of the above mentioned methods reduce the computation time of sparse DOA estimation algorithms, the computational complexity of the l_1-norm minimization is still relatively large. In [21,22], a fast sparse representation method, called smoothed l_0-norm algorithm was proposed. With the same or better accuracy, the minimization of smoothed l_0-norm can perform about two to three orders of magnitude faster than l_1-norm minimization [21–23]. This is because the smoothed l_0-norm method avoids the l_1-norm minimization, which is a convex optimization problem usually addressed by linear programming algorithms. More specifically, smoothed l_0-norm method approximates the l_0-norm by a smooth function, and then uses the graduated nonconvexity (GNC) approach [24] and the gradient-based methods to obtain the minimization. In the fields of imaging and power-line communications, smoothed l_0-norm algorithm has been applied [25,26]. However, to the best of our knowledge, to date there are no references about smoothed l_0-norm based DOA estimation methods.

In this paper, we propose a reweighted smoothed l_0-norm algorithm for DOA estimation in monostatic MIMO radar. The aim of this paper is to significantly reduce the computation time of the SR-based DOA estimation, and achieve better accuracy than the conventional l_1-norm minimization based methods. The novel method firstly performs the vectorization operation on the covariance matrix to form a covariance vector, where the covariance matrix is calculated from the latest data matrix obtained by a reduced dimensional transformation. Next, a weighted matrix is constructed to change the covariance estimation errors into a Gaussian white vector. Then, another reweighted vector is designed to enhance sparse solution. Finally, a reweighted smoothed l_0-norm minimization framework with a reweighted continuous function is designed, based on which the sparse solution is obtained by using a decreasing parameter sequence and the steepest ascent algorithm to achieve the DOA estimation. With enhanced smoothed estimation of the l_0-norm, the designed reweighted smoothed l_0-norm algorithm avoids the signal recovery problem of the l_1-norm constrained minimization. Compared with the conventional l_1-norm penalty based DOA estimation algorithms, such as l_1-SVD [9], reweighted l_1-SVD [18] and RV l_1-SRACV [20], the proposed method needs considerably less computation time. Meanwhile, it can achieve higher spatial angular resolution and better angle estimation performance.

Notation: $(\cdot)^{\mathrm{H}}$, $(\cdot)^{\mathrm{T}}$, $(\cdot)^{-1}$ and $(\cdot)^*$ denote conjugate-transpose, transpose, inverse and conjugate operators, respectively. $\otimes$ and $\odot$ denote the Kronecker and the Khatri-Rao product operators, respectively. $\mathbf{I}_K$ denotes a $K \times K$ dimensional unit matrix. $||\cdot||_0$, $||\cdot||_1$, $||\cdot||_2$ and $||\cdot||_F$ denote the l_0-norm, the l_1-norm, the l_2-norm and the Frobenius-norm, respectively. $\mathrm{vec}(\cdot)$ denotes the vectorization operator. $\mathrm{E}(\cdot)$ denotes the expectation operator.

2. System model

A narrowband monostatic MIMO radar system is considered. The transmit array and the receive array are both half-wavelength $\lambda/2$ spaced uniform linear arrays (ULAs), with M transmit antennas and N receive antennas. M different and mutually orthogonal narrowband waveforms with identical bandwidth and centre frequency are transmitted by the transmit antennas. In the far field, there are P uncorrelated targets assumed to be located at the same range bin. The targets are modeled as point scatterers, whose DOAs are $\theta_1, \theta_2, \dots, \theta_P$, respectively. In monostatic MIMO radar, the angles of DOD and DOA are considered as the same. The matched filtering is done only in range, additionally, it is assumed that the perfect point-spread function is able to be produced. Outputs are from the targets whose matched filtering has already been done. After all the matched filters, the outputs can be stacked into an $MN \times 1$ vector. As a consequence, at snapshot t, the received data vector $\mathbf{x}(t)$ is expressed as [7,8,20,27]

$$\mathbf{x}(t) = [\mathbf{a}_t(\theta_1) \otimes \mathbf{a}_r(\theta_1), \dots, \mathbf{a}_t(\theta_P) \otimes \mathbf{a}_r(\theta_P)]\mathbf{s}(t) + \mathbf{n}(t) \tag{1}$$

where $\mathbf{a}_t(\theta_p)$ and $\mathbf{a}_r(\theta_p)$ are the transmit and the receive steering vectors, respectively. More specifically, $\mathbf{a}_t(\theta_p) = [1, e^{j\pi \sin(\theta_p)}, e^{j\pi 2\sin(\theta_p)}, \dots, e^{j\pi (M-1)\sin(\theta_p)}]^{\mathrm{T}} \in \mathbb{C}^{M\times 1}$ and $\mathbf{a}_r(\theta_p) = [1, e^{j\pi \sin(\theta_p)}, e^{j\pi 2\sin(\theta_p)}, \dots, e^{j\pi (N-1)\sin(\theta_p)}]^{\mathrm{T}} \in \mathbb{C}^{N\times 1}$, $p = 1, 2, \dots, P$. $\mathbf{s}(t) = [s_1(t), s_2(t), \dots, s_P(t)]^{\mathrm{T}} \in \mathbb{C}^{P\times 1}$ is the zero-mean signal vector with $s_p(t) = \varrho_p(t)e^{j2\pi f_p t}$, in which $\varrho_p(t)$ and f_p are the reflection coefficient and Doppler frequency, respectively [7,8]. For the pth target, the Doppler frequency is assumed to be constant over the processing time. Different targets have different reflection coefficients, which are random and depend on the target radar cross section (RCS). The target model is considered as the classical Swerling case II, thus RCS fluctuations are constant during a snapshot period, and vary independently from snapshot to snapshot [27]. $\mathbf{n}(t) \in \mathbb{C}^{MN\times 1}$ is the Gaussian white noise vector with zero mean and covariance matrix $\tau^2\mathbf{I}_{MN}$. The noise is assumed to be statistically independent with the signals. Let $\mathbf{A} = [\mathbf{a}_t(\theta_1) \otimes \mathbf{a}_r(\theta_1), \dots, \mathbf{a}_t(\theta_P) \otimes \mathbf{a}_r(\theta_P)] \in \mathbb{C}^{MN\times P}$ be the steering matrix, by collecting J snapshots, the received data matrix is [18]

$$\mathbf{X} = \mathbf{AS} + \mathbf{N} \tag{2}$$

where $\mathbf{X} = [\mathbf{x}(1), \mathbf{x}(2), \dots, \mathbf{x}(J)] \in \mathbb{C}^{MN\times J}$. $\mathbf{S} = [\mathbf{s}(1), \mathbf{s}(2), \dots, \mathbf{s}(J)] \in \mathbb{C}^{P\times J}$ and $\mathbf{N} = [\mathbf{n}(1), \mathbf{n}(2), \dots, \mathbf{n}(J)] \in \mathbb{C}^{MN\times J}$ are the signal data matrix and the circular complex Gaussian white noise matrix, respectively. In the conventional l_1-norm based sparse DOA estimation methods such as l_1-SVD algorithm [9], the DOAs can be estimated by solving an l_1-norm minimization based sparse signal recovery problem with $O[L^3P]$ calculation burden [9,20], where L is the number of the discretized sampling grids in the complete dictionary, $L \gg P$. To considerably reduce the computational complexity of the DOA estimation that is based on sparse representation, in the following, we propose a reweighted smoothed l_0-norm algorithm for DOA estimation in MIMO radar.

3. Reweighted smoothed l_0-norm based sparse DOA estimation algorithm for monostatic MIMO radar

In each column of the steering matrix $\mathbf{A}$ in monostatic MIMO radar, $(M+N-1)$ elements are unique. Therefore, the model could be rearranged. Exploiting this feature, a reduced dimensional transformation is adopted to lower the dimension of the received data $\mathbf{X}$. The pth column in $\mathbf{A}$ can be expressed as $\mathbf{a}_t(\theta_p) \otimes \mathbf{a}_r(\theta_p) = \bar{\mathbf{J}}\mathbf{b}(\theta_p)$ [18] for $p = 1, 2, \dots, P$, where

$$\mathbf{b}(\theta_p) = [1, e^{j\pi \sin(\theta_p)}, e^{j\pi 2\sin(\theta_p)}, \dots, e^{j\pi (M+N-2)\sin(\theta_p)}]^{\mathrm{T}}$$
$$\bar{\mathbf{J}} = [\boldsymbol{\Upsilon}_0^{\mathrm{T}}, \boldsymbol{\Upsilon}_1^{\mathrm{T}}, \cdots, \boldsymbol{\Upsilon}_{M-1}^{\mathrm{T}}]^{\mathrm{T}} \tag{3}$$

with $\boldsymbol{\Upsilon}_m = [\mathbf{0}_{N\times m}, \mathbf{I}_N, \mathbf{0}_{N\times(M-m-1)}] \in \mathbb{C}^{N\times(M+N-1)}$ for $m = 0, 1, \ldots, M-1$. Note that $\mathbf{b}(\theta_p) \in \mathbb{C}^{(M+N-1)\times 1}$ and $\bar{\mathbf{J}} \in \mathbb{C}^{MN\times(M+N-1)}$. Then, we have

$$\mathbf{A} = \bar{\mathbf{J}}\mathbf{B} \tag{4}$$

where $\mathbf{B} = [\mathbf{b}(\theta_1), \mathbf{b}(\theta_2), \ldots, \mathbf{b}(\theta_P)] \in \mathbb{C}^{(M+N-1)\times P}$. Therefore, based on the relationship between $\mathbf{A}$ and $\mathbf{B}$, a reduced dimensional matrix can be defined as

$$\mathbf{T} = \mathbf{F}^{-1}\bar{\mathbf{J}}^{\mathrm{H}} \tag{5}$$

where $\mathbf{T} \in \mathbb{C}^{(M+N-1)\times MN}$, $\mathbf{F} = (\bar{\mathbf{J}}^{\mathrm{H}}\bar{\mathbf{J}})^{(\frac{1}{2})}$ is a diagonal matrix and directly calculated as

$$\mathbf{F} = \mathrm{diag}[1, \sqrt{2}, \ldots, \underbrace{\varepsilon, \ldots, \varepsilon}_{|M-N|+1}, \ldots, \sqrt{2}, 1] \tag{6}$$

with $\varepsilon = \min(\sqrt{M}, \sqrt{N})$. Consequently, utilizing $\mathbf{T}$ in Eq. (5), the reduced dimensional transformation of the data matrix $\mathbf{X}$ in Eq. (2) is implemented as follows

$$\begin{aligned}\bar{\mathbf{X}} &= \mathbf{F}^{-1}\bar{\mathbf{J}}^{\mathrm{H}}\bar{\mathbf{J}}\mathbf{B}\mathbf{S} + \mathbf{T}\mathbf{N} \\ &= \mathbf{F}\mathbf{B}\mathbf{S} + \bar{\mathbf{N}}\end{aligned} \tag{7}$$

where $\bar{\mathbf{X}} = \mathbf{T}\mathbf{X} \in \mathbb{C}^{(M+N-1)\times J}$ and $\bar{\mathbf{N}} = \mathbf{T}\mathbf{N} = [\bar{\mathbf{n}}(1), \bar{\mathbf{n}}(2), \ldots, \bar{\mathbf{n}}(J)] \in \mathbb{C}^{(M+N-1)\times J}$ are the new received data matrix and noise matrix, respectively. Since $\mathbf{T}\mathbf{T}^{\mathrm{H}} = \mathbf{I}_{M+N-1}$, according to the invariant feature of linear transformation in asymptotic normal distribution, $\bar{\mathbf{n}}(t)$ is the Gaussian vector with zero mean and covariance matrix $\mathbf{T}(\tau^2\mathbf{I}_{MN})\mathbf{T}^{\mathrm{H}} = \tau^2\mathbf{I}_{M+N-1}$, namely, $\bar{\mathbf{N}}$ is the Gaussian white noise matrix. The reduced dimensional transformation in Eq. (7) lower the dimension of data matrix from $MN \times J$ to $(M+N-1)\times J$.

After obtaining the new received data matrix $\bar{\mathbf{X}}$, the covariance matrix of $\bar{\mathbf{X}}$ can be represented as

$$\mathbf{R}_{\bar{X}} = \mathrm{E}(\bar{\mathbf{X}}\bar{\mathbf{X}}^{\mathrm{H}}) = \mathbf{F}\mathbf{B}\mathbf{R}_S(\mathbf{F}\mathbf{B})^{\mathrm{H}} + \mathbf{R}_{\bar{N}} \tag{8}$$

with the assumptions about the noise and the signals in Eq. (1). In Eq. (8), $\mathbf{R}_S = \mathrm{E}(\mathbf{S}\mathbf{S}^{\mathrm{H}}) = \mathrm{diag}[\rho_1^2, \rho_2^2, \ldots, \rho_P^2]$ and $\mathbf{R}_{\bar{N}} = \mathrm{E}(\bar{\mathbf{N}}\bar{\mathbf{N}}^{\mathrm{H}}) = \mathrm{diag}[\tau_1^2, \tau_2^2, \ldots, \tau_{M+N-1}^2]$ are the signal and the noise covariance matrices, respectively. $\{\rho_p^2\}_{p=1}^P$ is the signal power corresponding to the P targets and $\{\tau_i^2\}_{i=1}^{M+N-1}$ is the noise power. As the pth diagonal element ρ_p^2 in $\mathbf{R}_S$ is $\rho_p^2 = \mathrm{E}[\mathbf{S}(p,:)\mathbf{S}(p,:)^{\mathrm{H}}]$, ρ_p is related to $\varrho_p(t)$ and $\rho_p^2 = \frac{1}{J}\sum_{t=1}^{J}\varrho_p(t)\varrho_p(t)^*$. According to the properties of vectorization operator, the vectorization of $\mathbf{R}_{\bar{X}}$ can be exploited to enlarge the array aperture, which is expressed as

$$\bar{\mathbf{y}}_v = [(\mathbf{F}\mathbf{B})^* \otimes (\mathbf{F}\mathbf{B})]\mathrm{vec}(\mathbf{R}_S) + \mathrm{vec}(\mathbf{R}_{\bar{N}}) \tag{9}$$

where $\bar{\mathbf{y}}_v = \mathrm{vec}(\mathbf{R}_{\bar{X}}) \in \mathbb{C}^{(M+N-1)^2\times 1}$. Since $\mathbf{R}_s$ is a diagonal matrix, the non-zero values in $\mathrm{vec}(\mathbf{R}_S)$ correspond to the non-zero diagonal elements in $\mathbf{R}_S$. Thus, $\bar{\mathbf{y}}_v$ can be derived as

$$\bar{\mathbf{y}}_v = [(\mathbf{F}\mathbf{B})^* \odot (\mathbf{F}\mathbf{B})]\mathbf{y}_s + \bar{\mathbf{y}}_n \tag{10}$$

where $\mathbf{y}_s = [\rho_1^2, \rho_2^2, \ldots, \rho_P^2]^{\mathrm{T}} \in \mathbb{C}^{P\times 1}$, and $\bar{\mathbf{y}}_n = \mathrm{vec}(\mathbf{R}_{\bar{N}}) \in \mathbb{C}^{(M+N-1)^2\times 1}$. With Eq. (10), sparse representation scheme can be applied to achieve the DOA estimation by first constructing a complete dictionary, which contains much more potential DOAs than the actual DOAs of the targets. By slicing the continuous range of possible incident angles into L cells, we can obtain an angle grid $\{\hat{\theta}_i\}_{i=1}^L$ to represent a series of discretized directions of all interested DOAs [14]. Note that since $\{\hat{\theta}_i\}_{i=1}^L$ are with respect to all possible target locations, L is typically much larger than the target number P, i.e. $L \gg P$ [9]. Super-resolution sparse DOA estimation methods are able to resolve sources within a Rayleigh cell, and overcome the Rayleigh resolution limit $\Delta\gamma$ [28], i.e. the beamwidth in the spatial frequency space, defined as the full width of the mainlobe at the half-power level and calculated as $\Delta\gamma = \frac{0.886}{\bar{l}_a/\lambda}$ [29], where $\bar{l}_a$ is the effective array aperture and λ is the wavelength. Thus, the grid cell size should be smaller than $\Delta\gamma$. Furthermore, the setting of the cell size should be reasonable small so that we can assume that the targets just happen to be located at the cells within the desired accuracy, namely, they are considered to be on-grid. The dictionary is obtained by calculating

$$\Omega_{\hat{\theta}} = (\mathbf{F}\mathbf{B}_{\hat{\theta}}^*) \odot (\mathbf{F}\mathbf{B}_{\hat{\theta}}) \tag{11}$$

with $\mathbf{B}_{\hat{\theta}} = [\mathbf{b}(\hat{\theta}_1), \mathbf{b}(\hat{\theta}_2), \ldots, \mathbf{b}(\hat{\theta}_L)] \in \mathbb{C}^{(M+N-1)\times L}$. After obtaining $\Omega_{\hat{\theta}}$, assume that a sparse vector $\mathbf{y}_s^{\hat{\theta}} \in \mathbb{C}^{L\times 1}$ can be formulated to satisfy $\bar{\mathbf{y}}_v = \Omega_{\hat{\theta}}\mathbf{y}_s^{\hat{\theta}} + \bar{\mathbf{y}}_n$, so that $\mathbf{y}_s^{\hat{\theta}}$ and $\mathbf{y}_s$ have the same row support. It indicates that the elements in $\mathbf{y}_s^{\hat{\theta}}$ are nonzero only when they correspond to the actual target DOAs, and then DOA estimation can be viewed as finding out the nonzero values in $\mathbf{y}_s^{\hat{\theta}}$. To solve the sparse recovery problem by counting the smallest number of the nonzero elements of $\mathbf{y}_s^{\hat{\theta}}$, an ideal sparse metric is the l_0-norm penalty, which can be expressed as

$$\min_{\mathbf{y}_s^{\hat{\theta}}} \| \mathbf{y}_s^{\hat{\theta}} \|_0, \quad \text{s.t.} \quad \bar{\mathbf{y}}_v = \Omega_{\hat{\theta}}\mathbf{y}_s^{\hat{\theta}} + \bar{\mathbf{y}}_n \tag{12}$$

Based on Eq. (12), the spatial spectrum can be obtained by finding the sparse solution of $\mathbf{y}_s^{\hat{\theta}}$. However, solving the l_0-norm minimization based sparse recovery problem in Eq. (12) is non-convex and NP-hard. To avoid the l_0-norm minimization, the approximate penalty called l_1-norm minimization is widely used in sparse representation-based DOA estimation methods [9,10,16–20]. In order to reduce the computational complexity and achieve better estimation performance, by designing a new reweighted algorithm based on smoothed l_0-norm, a reweighted smoothed l_0-norm based DOA estimation method is proposed in the following. The l_0-norm in Eq. (12) is the number of non-zero elements of $\mathbf{y}_s^{\hat{\theta}} = [y_{s1}^{\hat{\theta}}, y_{s2}^{\hat{\theta}}, \ldots, y_{sL}^{\hat{\theta}}]$, which can be represented as follows

$$||\mathbf{y}_s^{\hat{\theta}}||_0 = \sum_{i=1}^{L} \upsilon(y_{si}^{\hat{\theta}}) \tag{13}$$

where $\upsilon(y_{si}^{\hat{\theta}})$ is defined as

$$\upsilon(y_{si}^{\hat{\theta}}) = \begin{cases} 1 & y_{si}^{\hat{\theta}} \neq 0 \\ 0 & y_{si}^{\hat{\theta}} = 0 \end{cases} \tag{14}$$

Since $\upsilon(y_{si}^{\hat{\theta}})$ is discontinuous, l_0-norm is discontinuous. The viewpoint of the proposed reweighted smoothed l_0-norm is to approximate the l_0-norm by designing a continuous function with reweighted coefficients, then the reweighted smoothed estimation of l_0-norm can be obtained. This enables us to utilize the gradient-based methods to gain the minimization and solve the problem of high noise sensitivity of the l_0-norm. For obtaining the reweighted coefficients, firstly, the singular value decomposition (SVD) of $\mathbf{R}_{\bar{X}}$ is applied to extract the noise subspace $\mathbf{U}_n$. That is $\mathbf{R}_{\bar{X}} = \mathbf{U}\boldsymbol{\Lambda}\mathbf{V}^{\mathrm{H}}$, in which $\boldsymbol{\Lambda} = \mathrm{diag}[\omega_1, \omega_2, \ldots, \omega_{M+N-1}]$ with $\omega_1 \geq \omega_2 \geq \cdots \geq \omega_{M+N-1}$ being the singular values, and $\mathbf{U}_n$ is made up of the $(M+N-1-P)$ columns in $\mathbf{U}$ that correspond to $(\omega_{P+1}, \omega_{P+2}, \ldots, \omega_{M+N-1})$. Then based on Eq. (7) and the orthogonality between the steering vector $\mathbf{F}\mathbf{b}(\theta_p)$ and the noise subspace $\mathbf{U}_n \in \mathbb{C}^{(M+N-1)\times(M+N-1-P)}$, the reweighted vector is designed as

$$\mathbf{r}_w = [(\mathbf{F}\mathbf{B}_{\hat{\theta}})^{\mathrm{H}}\mathbf{U}_n]^{(l_2)} / \max\{[(\mathbf{F}\mathbf{B}_{\hat{\theta}})^{\mathrm{H}}\mathbf{U}_n]^{(l_2)}\} \tag{15}$$

where $[(\mathbf{F}\mathbf{B}_{\hat{\theta}})^{\mathrm{H}}\mathbf{U}_n]^{(l_2)} \in \mathbb{C}^{L\times 1}$ stands for a vector whose ith element is equal to the l_2-norm of the ith row in $(\mathbf{F}\mathbf{B}_{\hat{\theta}})^{\mathrm{H}}\mathbf{U}_n$. According to the subspace theorem [6], for the true target DOA θ_p, $[(\mathbf{F}\mathbf{b}(\theta_p))^{\mathrm{H}}\mathbf{U}_n]^{(l_2)} \to 0$ when $J \to \infty$. Since $\mathbf{F}\mathbf{B}_{\hat{\theta}}$ contains the P steering vectors in relation to the actual targets, $\mathbf{r}_w$ is divided into the following two parts: $\mathbf{r}_w^1$ that corresponds to the true DOAs, and $\mathbf{r}_w^2$ that consists of the remaining elements in $\mathbf{r}_w$. As a result, the values in $\mathbf{r}_w^1$ and $\mathbf{r}_w^2$ satisfy $\mathbf{r}_w^1(p) \to 0$ and $0 < \mathbf{r}_w^2(j) \le 1$, respectively, and $\mathbf{r}_w^1(p) < \mathbf{r}_w^2(j)$. The reweighted vector $\mathbf{r}_w$ can be written as $\mathbf{r}_w = [r_{w1}, r_{w2}, \ldots, r_{wL}]^{\mathrm{T}}$ with r_{wi} being the reweighted coefficient, $i = 1, 2, \ldots, L$. For the reweighted smoothed estimation of the l_0-norm in Eq. (13), the continuous function with reweighted coefficients is designed as follows

$$f_\sigma(r_{wi}, y_{si}^{\hat\theta}) = r_{wi} e^{-|y_{si}^{\hat\theta}|^2/2\sigma^2} \tag{16}$$

for $i = 1, 2, \ldots, L$, and r_{wi} is obtained from Eq. (15). Thus, $\upsilon(y_{si}^{\hat\theta})$ can be substituted by $f_\sigma(r_{wi}, y_{si}^{\hat\theta})$, that is

$$\lim_{\sigma\to 0} f_\sigma(r_{wi}, y_{si}^{\hat\theta}) = \begin{cases} 1 & r_{wi} = 1, y_{si}^{\hat\theta} = 0 \\ 0 & r_{wi} = 0, y_{si}^{\hat\theta} \neq 0 \end{cases} \tag{17}$$

or

$$f_\sigma(r_{wi}, y_{si}^{\hat\theta}) \approx \begin{cases} 1 & r_{wi} \to 1, \mid y_{si}^{\hat\theta} \mid \ll \sigma \\ 0 & r_{wi} \to 0, \mid y_{si}^{\hat\theta} \mid \gg \sigma \end{cases} \tag{18}$$

According to Eq. (13) and Eq. (18), $\upsilon(y_{si}^{\hat\theta}) \approx 1 - f_\sigma(r_{wi}, y_{si}^{\hat\theta})$ with small σ can be exploited to gain the approximation of the l_0-norm. Furthermore, it can be observed in Eq. (18) that for the true target DOA θ_p, the corresponding solution $y_{sp}^{\hat\theta}$ and the reweighted coefficient r_{wp} satisfy $\mid y_{sp}^{\hat\theta} \mid \gg \sigma$ and $r_{wp} \to 0$ simultaneously. Hence, the designed reweighted continuous function $f_\sigma(r_{wi}, y_{si}^{\hat\theta})$ enhances the approximation relationship between $\upsilon(y_{si}^{\hat\theta})$ and $1 - f_\sigma(r_{wi}, y_{si}^{\hat\theta})$, which can further enhance the smoothed estimation of the l_0-norm solution. Then Eq. (13) can be rewritten as

$$||\mathbf{y}_s^{\hat\theta}||_0 \approx L - F_\sigma(\mathbf{r}_w, \mathbf{y}_s^{\hat\theta}) \tag{19}$$

with

$$F_\sigma(\mathbf{r}_w, \mathbf{y}_s^{\hat\theta}) = \sum_{i=1}^{L} f_\sigma(r_{wi}, y_{si}^{\hat\theta}) \tag{20}$$

where $F_\sigma(\mathbf{r}_w, \mathbf{y}_s^{\hat\theta})$ measures the sparsity of $\mathbf{y}_s^{\hat\theta}$. The sparser $\mathbf{y}_s^{\hat\theta}$ is, the larger $F_\sigma(\mathbf{r}_w, \mathbf{y}_s^{\hat\theta})$ will be. This indicates that achieving the minimization of the l_0-norm can be regarded as maximizing $F_\sigma(\mathbf{r}_w, \mathbf{y}_s^{\hat\theta})$ that satisfies Eq. (12). Therefore, with the enhanced approximation between $||\mathbf{y}_s^{\hat\theta}||_0$ and $L - F_\sigma(\mathbf{r}_w, \mathbf{y}_s^{\hat\theta})$, the reweighted smoothed l_0-norm based sparse representation framework is designed as

$$\max_{\mathbf{y}_s^{\hat\theta}} F_\sigma(\mathbf{r}_w, \mathbf{y}_s^{\hat\theta}), \quad \text{s.t.} \quad \bar{\mathbf{y}}_{vn} = \Omega_{\hat\theta}\mathbf{y}_s^{\hat\theta} \tag{21}$$

with $\sigma \to 0$ and $\bar{\mathbf{y}}_{vn} = (\bar{\mathbf{y}}_v - \bar{\mathbf{y}}_n) \in \mathbb{C}^{(M+N-1)^2\times 1}$. The selected value of σ adjusts the smoothness and the accuracy of the approximation in Eq. (19). When σ is small enough, $L - F_\sigma(\mathbf{r}_w, \mathbf{y}_s^{\hat\theta})$ is close enough to the true value of the l_0-norm, however, it contains lots of local maxima. With σ increasing, the reweighted smoothed l_0-norm becomes smoother. Thus with less local maxima, obtaining its solution gets faster, but the accuracy is degraded. To guarantee the solution speed and the accuracy simultaneously, the idea of decreasing σ gradually in a reasonable sequence $\sigma = [\sigma_1, \sigma_2, \ldots, \sigma_K]$ can be adopted for DOA estimation of Eq. (21). In addition, for each value of σ in the sequence, the steepest ascent algorithm is exploited to gain the maximization of $F_\sigma(\mathbf{r}_w, \mathbf{y}_s^{\hat\theta})$ on the affine set $\mathcal{Y} = \{\mathbf{y}_s^{\hat\theta} \mid \bar{\mathbf{y}}_{vn} = \Omega_{\hat\theta}\mathbf{y}_s^{\hat\theta}\}$.

When implementing the steepest ascent algorithm for σ_{k+1}, the initial value in demand is obtained from the solution of maximizing $F_\sigma(\mathbf{r}_w, \mathbf{y}_s^{\hat\theta})$ in Eq. (21) with $\sigma = \sigma_k$. To start the steepest ascent algorithm with σ_1, the initialization can be set as finding the solution of Eq. (21) with $\sigma \to \infty$. It has been pointed out that it is the minimum l_2-norm solution when $\sigma \to \infty$ [30]. Hence, the value of initialization is calculated by

$$(\mathbf{y}_s^{\hat\theta})_0 = \Omega_{\hat\theta}^{+}\bar{\mathbf{y}}_{vn} \tag{22}$$

where $\Omega_{\hat\theta}^{+}$ denotes the pseudo-inverse of $\Omega_{\hat\theta}$, and $\Omega_{\hat\theta}^{+} = (\Omega_{\hat\theta}^{\mathrm{H}})(\Omega_{\hat\theta}\Omega_{\hat\theta}^{\mathrm{H}})^{-1} \in \mathbb{C}^{L\times(M+N-1)^2}$. Then, each value of σ in the decreasing sequence $[\sigma_1, \sigma_2, \ldots, \sigma_K]$ is set down. σ_1 can be chosen as one to four times of $\max\{(\mathbf{y}_s^{\hat\theta})_0\}$, in which $\max\{(\mathbf{y}_s^{\hat\theta})_0\}$ is the maximizer in the vector $(\mathbf{y}_s^{\hat\theta})_0 \in \mathbb{C}^{L\times 1}$. σ_K is set as a small value determined by the desired accuracy [21,22]. For the σ sequence, a factor can be adopted to decrease σ gradually, namely, the relationship between σ_{k+1} and σ_k is $\sigma_{k+1} = \alpha\sigma_k$.

In the steepest ascent algorithm with $\sigma = \sigma_k$, Q iterations are used to achieve the maximization of $F_\sigma(\mathbf{r}_w, \mathbf{y}_s^{\hat\theta})$ in Eq. (21). During each iteration, $\mathbf{y}_s^{\hat\theta} \leftarrow \mathbf{y}_s^{\hat\theta} + \bar\mu \nabla F_\sigma(\mathbf{r}_w, \mathbf{y}_s^{\hat\theta})$ is calculated with $\bar\mu$ being a step-size parameter. Since $\bar\mu$ should be decreasing with the decrease of σ [21], we set $\bar\mu = \mu\sigma^2$. Thus, we further have $\mathbf{y}_s^{\hat\theta} \leftarrow \mathbf{y}_s^{\hat\theta} + \mu\sigma^2 \nabla F_\sigma(\mathbf{r}_w, \mathbf{y}_s^{\hat\theta}) = \mathbf{y}_s^{\hat\theta} - \mu \triangle \mathbf{y}_s^{\hat\theta}$, in which μ is a positive constant and $\triangle \mathbf{y}_s^{\hat\theta}$ is represented as

$$\triangle \mathbf{y}_s^{\hat\theta} = [r_{w1}y_{s1}^{\hat\theta}e^{-|y_{s1}^{\hat\theta}|^2/2\sigma^2}, r_{w2}y_{s2}^{\hat\theta}e^{-|y_{s2}^{\hat\theta}|^2/2\sigma^2}, \ldots, r_{wL}y_{sL}^{\hat\theta}e^{-|y_{sL}^{\hat\theta}|^2/2\sigma^2}] \tag{23}$$

Then, this iteration projects $\mathbf{y}_s^{\hat\theta}$ back to the feasible set $\mathcal{Y}$, that is

$$\mathbf{y}_s^{\hat\theta} \leftarrow \mathbf{y}_s^{\hat\theta} - \Omega_{\hat\theta}^{+}[\Omega_{\hat\theta}\mathbf{y}_s^{\hat\theta} - \bar{\mathbf{y}}_{vn}] \tag{24}$$

After computing the Q iterations with $\sigma = \sigma_k$, we start the steepest ascent algorithm for $\sigma = \sigma_{k+1}$. The final sparse solution is the output of the steepest ascent algorithm for $\sigma = \sigma_K$.

In practical applications, the covariance matrix $\mathbf{R}_{\bar X}$ is estimated from J snapshots, i.e. $\hat{\mathbf{R}}_{\bar X} = \bar{\mathbf{X}}\bar{\mathbf{X}}^{\mathrm{H}}/J$. Thus, the estimation errors of $\mathbf{R}_{\bar X}$ may cause some noises. However, it has been verified that when the noise is an additive white Gaussian noise, the sparse method of obtaining the smoothed solution can be well applied to the noisy case [22,24,26]. Let $\Delta\mathbf{R}_{\bar X} = \hat{\mathbf{R}}_{\bar X} - \mathbf{R}_{\bar X}$ be the estimation error matrix of $\mathbf{R}_{\bar X}$. It has been pointed out that the elements in $\Delta\mathbf{R}_{\bar X}$ comply with the following distribution [31]

$$\mathrm{vec}(\Delta\mathbf{R}_{\bar X}) \sim \mathrm{AsN}\left(0, \frac{1}{J}\mathbf{R}_{\bar X}^{\mathrm{T}} \otimes \mathbf{R}_{\bar X}\right) \tag{25}$$

where $\mathrm{AsN}(\mu, \mathbf{C})$ denotes asymptotic normal distribution with μ and $\mathbf{C}$ being the mean and the covariance matrix, respectively. The asymptotic standard normal distribution can be obtained with a weighted matrix $\mathbf{W}^{-\frac{1}{2}} = \sqrt{J}\mathbf{R}_{\bar X}^{-\frac{\mathrm{T}}{2}} \otimes \mathbf{R}_{\bar X}^{-\frac{1}{2}}$, based on which the sparse representation framework in Eq. (12) can transform into

$$\min_{\mathbf{y}_s^{\hat\theta}} \| \mathbf{y}_s^{\hat\theta} \|_0, \quad \text{s.t.} \quad \mathbf{W}^{-\frac{1}{2}}(\hat{\bar{\mathbf{y}}}_v - \bar{\mathbf{y}}_n) = \mathbf{W}^{-\frac{1}{2}}\Omega_{\hat\theta}\mathbf{y}_s^{\hat\theta} + \Delta\mathbf{e} \tag{26}$$

where $\hat{\bar{\mathbf{y}}}_v = \mathrm{vec}(\hat{\mathbf{R}}_{\bar X}) \in \mathbb{C}^{(M+N-1)^2\times 1}$, and $\Delta\mathbf{e} = \mathbf{W}^{-\frac{1}{2}}\mathrm{vec}(\Delta\mathbf{R}_{\bar X})$ is the new Gaussian white error vector. Therefore, the final reweighted smoothed l_0-norm based sparse representation framework is designed as follows

$$\max_{\mathbf{y}_s^{\hat\theta}} F_\sigma(\mathbf{r}_w, \mathbf{y}_s^{\hat\theta}), \quad \text{s.t.} \quad \tilde{\mathbf{y}}_w = \tilde\Omega_{\hat\theta}\mathbf{y}_s^{\hat\theta} + \Delta\mathbf{e} \tag{27}$$

where $\tilde{\mathbf{y}}_w = \mathbf{W}^{-\frac{1}{2}}(\hat{\bar{\mathbf{y}}}_v - \bar{\mathbf{y}}_n) \in \mathbb{C}^{(M+N-1)^2\times 1}$ is the new observation vector, $\tilde\Omega_{\hat\theta} = \mathbf{W}^{-\frac{1}{2}}\Omega_{\hat\theta} \in \mathbb{C}^{(M+N-1)^2\times L}$ is the new complete dictionary. $F_\sigma(\mathbf{r}_w, \mathbf{y}_s^{\hat\theta})$ is designed as Eq. (16) and Eq. (20), and its reweighted coefficients are defined in Eq. (15). The estimation of $\bar{\mathbf{y}}_n$

Table 1
The proposed reweighted smoothed l_0-norm algorithm for DOA estimation.

Step 1	Implement the reduced dimensional transformation of received data matrix as Eq. (7). Then calculate the covariance matrix from J snapshots, i.e. $\hat{\mathbf{R}}_{\bar{X}} = \bar{\mathbf{X}}\bar{\mathbf{X}}^{\mathrm{H}}/J$.
Step 2	Perform the vectorization operation on $\hat{\mathbf{R}}_{\bar{X}}$, i.e. $\hat{\bar{\mathbf{y}}}_v = \mathrm{vec}(\hat{\mathbf{R}}_{\bar{X}})$, and define the weighted matrix as $\mathbf{W}^{-\frac{1}{2}} = \sqrt{J}\hat{\mathbf{R}}_{\bar{X}}^{-\frac{\mathrm{T}}{2}} \otimes \hat{\mathbf{R}}_{\bar{X}}^{-\frac{1}{2}}$. Construct the complete dictionary as $\tilde{\Omega}_{\hat{\theta}} = \mathbf{W}^{-\frac{1}{2}}[(\mathbf{FB}_{\hat{\theta}}^{*}) \odot (\mathbf{FB}_{\hat{\theta}})]$ and the observation vector as $\tilde{\mathbf{y}}_w = \mathbf{W}^{-\frac{1}{2}}(\hat{\bar{\mathbf{y}}}_v - \hat{\bar{\mathbf{y}}}_n)$.
Step 3	Perform the SVD of $\hat{\mathbf{R}}_{\bar{X}}$, the reweighted vector is formulated as $\mathbf{r}_w = [(\mathbf{FB}_{\hat{\theta}})^{\mathrm{H}}\mathbf{U}_n]^{(l_2)}/\max\{[(\mathbf{FB}_{\hat{\theta}})^{\mathrm{H}}\mathbf{U}_n]^{(l_2)}\}$.
Step 4	Design the continuous function with reweighted coefficients as $f_\sigma(r_{wi}, y_{si}^{\hat{\theta}}) = r_{wi}e^{-\lvert y_{si}^{\hat{\theta}}\rvert^2/2\sigma^2}$, and then the reweighted smoothed l_0-norm based sparse representation framework as Eq. (27).
Step 5	Solve the final reweighted smoothed l_0-norm minimization problem for DOA estimation as follows: – Initialization a) Find a solution on the feasible set $\mathcal{Y}_\varepsilon$, such as the minimum l_2-norm solution $\mathbf{v}_0 = \tilde{\Omega}_{\hat{\theta}}^{+}\tilde{\mathbf{y}}_w$ for $\tilde{\mathbf{y}}_w = \tilde{\Omega}_{\hat{\theta}}\mathbf{y}_s^{\hat{\theta}}$. b) Set a reasonable decreasing sequence for σ, that is $\sigma = [\sigma_1, \sigma_2, \ldots, \sigma_K]$. σ_1 can be chosen as one to four times of $\max\{\lvert\mathbf{v}_0\rvert\}$. – For $k = 1, 2, \ldots, K$ a) Let $\sigma = \sigma_k$. b) Perform Q iterations to maximize $\mathcal{F}_\sigma(\mathbf{r}_w, \mathbf{y}_s^{\hat{\theta}})$ on feasible set $\tilde{\mathbf{y}}_w = \tilde{\Omega}_{\hat{\theta}}\mathbf{y}_s^{\hat{\theta}}$: i. Set $\mathbf{y}_s^{\hat{\theta}} = \mathbf{v}_{k-1}$. ii. For $q = 1, 2, \ldots, Q$ A. Calculate $\triangle\mathbf{y}_s^{\hat{\theta}} = [r_{w1}y_{s1}^{\hat{\theta}}e^{-\lvert y_{s1}^{\hat{\theta}}\rvert^2/2\sigma^2}, r_{w2}y_{s2}^{\hat{\theta}}e^{-\lvert y_{s2}^{\hat{\theta}}\rvert^2/2\sigma^2}, \ldots, r_{wL}y_{sL}^{\hat{\theta}}e^{-\lvert y_{sL}^{\hat{\theta}}\rvert^2/2\sigma^2}]$. B. Calculate $\mathbf{y}_s^{\hat{\theta}} \leftarrow \mathbf{y}_s^{\hat{\theta}} - \mu\triangle\mathbf{y}_s^{\hat{\theta}}$. C. Project $\mathbf{y}_s^{\hat{\theta}}$ back to the feasible set $\mathcal{Y}_\varepsilon$, that is $\mathbf{y}_s^{\hat{\theta}} \leftarrow \mathbf{y}_s^{\hat{\theta}} - \tilde{\Omega}_{\hat{\theta}}^{+}[\tilde{\Omega}_{\hat{\theta}}\mathbf{y}_s^{\hat{\theta}} - \tilde{\mathbf{y}}_w]$. c) Let $\mathbf{v}_k = \mathbf{y}_s^{\hat{\theta}}$. – The final solution is $\mathbf{y}_s^{\hat{\theta}} = \mathbf{v}_K$.
Step 6	The DOAs of targets are obtained by searching the spectrum of $\mathbf{y}_s^{\hat{\theta}}$.

can be obtained from $\hat{\bar{\mathbf{y}}}_n = \hat{\tau}^2\mathrm{vec}(\mathbf{I}_{M+N-1})$, where the noise power $\hat{\tau}^2$ is estimated by the average of the $M+N-1-P$ smallest eigenvalues of the covariance matrix $\hat{\mathbf{R}}_{\bar{X}}$.

In fact, if we define $\Delta\tilde{\mathbf{e}} = \tilde{\Omega}_{\hat{\theta}}^{+}\Delta\mathbf{e} = (\tilde{\Omega}_{\hat{\theta}}^{\mathrm{H}})(\tilde{\Omega}_{\hat{\theta}}\tilde{\Omega}_{\hat{\theta}}^{\mathrm{H}})^{-1}\Delta\mathbf{e}$ in Eq. (27), $\tilde{\mathbf{y}}_w = \tilde{\Omega}_{\hat{\theta}}\mathbf{y}_s^{\hat{\theta}} + \Delta\mathbf{e} = \tilde{\Omega}_{\hat{\theta}}\mathbf{y}_s^{\hat{\theta}} + \tilde{\Omega}_{\hat{\theta}}\Delta\tilde{\mathbf{e}} = \tilde{\Omega}_{\hat{\theta}}\tilde{\mathbf{y}}_s^{\hat{\theta}}$ can be obtained. Then we have $\tilde{\mathbf{y}}_s^{\hat{\theta}} \triangleq \mathbf{y}_s^{\hat{\theta}} + \Delta\tilde{\mathbf{e}}$ with $\mathbf{y}_s^{\hat{\theta}} \in \mathcal{Y}_\varepsilon = \{\mathbf{y}_s^{\hat{\theta}} \mid \|\tilde{\mathbf{y}}_w - \tilde{\Omega}_{\hat{\theta}}\mathbf{y}_s^{\hat{\theta}}\|_2 \le \varepsilon\}$, where ε is a positive number determined by the distribution of $\Delta\mathbf{e}$ [22,24,26]. Eq. (25) and Eq. (26) indicate that with reasonable number of snapshots, $\hat{\mathbf{R}}_{\bar{X}}$ and $\tilde{\mathbf{y}}_s^{\hat{\theta}}$ are close enough to $\mathbf{R}_{\bar{X}}$ and $\mathbf{y}_s^{\hat{\theta}}$. As a result, the previous reweighted smoothed l_0-norm algorithm for Eq. (21) is suitable for Eq. (27). Finally, by solving the sparse recovery problem in Eq. (27) with Eq. (22)–(24), the DOAs of targets are obtained. The proposed reweighted smoothed l_0-norm algorithm for DOA estimation is summarized in Table 1.

4. Related remarks

Remark 1. The computational complexity of the proposed DOA estimation algorithm is analyzed in the following. The main calculation burden of the proposed method is constructing the reweighted vector $\mathbf{r}_w$ as Eq. (15) and obtaining the sparse solution of the reweighted smoothed l_0-norm based sparse signal recovery problem in Eq. (27). The former needs $O[(M+N-1)(M+N-1-P)L_1]$, which indicates that when constructing $\mathbf{r}_w$, more targets can reduce the complexity because of the dimensional reduction of the noise subspace $\mathbf{U}_n$. The latter requires $O[(M+N-1)^2L_1QK]$ with Q iterations for $\sigma = [\sigma_1, \sigma_2, \ldots, \sigma_K]$, where L_1 is the total number of the discretized sample grid cells. Therefore, the complexity of the proposed algorithm is $O[(M+N-1)(M+N-1-P)L_1 + (M+N-1)^2L_1QK]$. Let $\bar{U} = M+N-1$, the computational complexities of different sparse representation-based DOA estimation algorithms are given in Table 2. Since $L_1 \gg \max\{P, \bar{U}, J, Q, K\}$, $O[2\bar{U}^2J + \frac{1}{4}L_1^3] \gg O[\bar{U}(\bar{U}-P)L_1 + \bar{U}^2L_1QK]$, which means that the calculation burden of the proposed method is significantly lower than that of l_1-SVD [9], reweighted l_1-SVD [18] and RV l_1-SRACV [20] algorithms. The proposed method performs the steepest ascent algorithm for each value in the σ decreasing sequence, and it avoids the conventional l_1-norm minimization based sparse signal recovery problem for DOA estimation. Consequently, the proposed method requires considerably less computation time than conventional sparse representation-based DOA estimation algorithms.

Table 2
The computational complexities of different DOA estimation algorithms.

Algorithm	Computational Complexity
l_1-SVD	$O[L_1^3P]$
Reweighted l_1-SVD	$O[\bar{U}^2L_1 + L_1^3P]$
RV l_1-SRACV	$O[2\bar{U}^2J + \frac{1}{4}L_1^3]$
Proposed Method	$O[\bar{U}(\bar{U}-P)L_1 + \bar{U}^2L_1QK]$

Remark 2. The detailed settings of parameters are concluded as follows. For the decreasing sequence $\sigma = [\sigma_1, \sigma_2, \ldots, \sigma_K]$, if $\sigma > 4\max\{\lvert\mathbf{v}_0\rvert\}$, we have $e^{-\lvert y_{si}^{\hat{\theta}}\rvert^2/2\sigma^2} > 0.96 \approx 1$, which indicates that in terms of $e^{-\lvert y_{si}^{\hat{\theta}}\rvert^2/2\sigma^2}$ in the reweighted continuous function $f_\sigma(r_{wi}, y_{si}^{\hat{\theta}})$, this value of σ acts virtually like infinity for all elements in the initialization solution [21,22,26]. Thus, σ_1 can be set as one to four times of the maximum absolute value in $\mathbf{v}_0 = \tilde{\Omega}_{\hat{\theta}}^{+}\tilde{\mathbf{y}}_w$. After that, a decreasing factor α can be exploited to decrease σ gradually, that is $\sigma_{k+1} = \alpha\sigma_k$, and in general, $0.5 \le \alpha \le 1$. The smallest σ can be chosen as about one to two times of the standard deviation of $\Delta\tilde{\mathbf{e}} = \tilde{\Omega}_{\hat{\theta}}^{+}\Delta\mathbf{e}$, for in this case, $e^{-\lvert y_{si}^{\hat{\theta}}\rvert^2/2\sigma^2}$ treats the elements in $\Delta\tilde{\mathbf{e}}$ as zeros [22]. Since $\Delta\mathbf{e}$ is the standard normal distribution, the covariance matrix of $\Delta\tilde{\mathbf{e}} \triangleq \tilde{\mathbf{y}}_s^{\hat{\theta}} - \mathbf{y}_s^{\hat{\theta}}$ is derived as $\tilde{\Omega}_{\hat{\theta}}^{+}(\mathbf{I}_L)(\tilde{\Omega}_{\hat{\theta}}^{+})^{\mathrm{H}}$. Besides, for the iterations of the steepest ascent algorithm, we just need a region near the maximizer of $\lvert\mathcal{F}_\sigma(\mathbf{r}_w, \mathbf{y}_s^{\hat{\theta}})\rvert$, thus a fixed small positive integer is applicable for Q. In each iteration, the choice $\mu \ge 1$ is reasonable [22].

Remark 3. The prior knowledge of the target number P affects the construction of the reweighted vector $\mathbf{r}_w$ and the reweighted continuous function $\mathcal{F}_\sigma(\mathbf{r}_w, \mathbf{y}_s^{\hat{\theta}})$. In practice, the perfect knowledge of P is not trivial to obtain. Moreover, it could vary over time. However, when necessary, several methods such as Akaike information criterion (AIC) and minimum description length (MDL) [32] can be applied to estimate P. In this paper, P is assumed to be known.

Remark 4. For the proposed algorithm, the maximum number of the targets that can be detected is analyzed as follows. By the reduced dimensional transformation, the steering matrix is changed from $\mathbf{A} \in \mathbb{C}^{MN\times P}$ to $\mathbf{FB} \in \mathbb{C}^{(M+N-1)\times P}$. Then we can conclude that in the dictionary $\tilde{\Omega}_{\hat{\theta}}$, any set of the $2(M+N-1)-1$ columns are independent [33]. It means the smallest number of the linearly dependent columns in $\tilde{\Omega}_{\hat{\theta}}$ is $2(M+N-1)$, which is expressed as $\text{Spark}(\tilde{\Omega}_{\hat{\theta}}) = 2(M+N-1)$. As discussed in [34,35], when the sparse recovery encounters the single measurement vector (SMV) problem, in order to uniquely determine the P-sparse vector $\mathbf{y}_s^{\hat{\theta}}$ for $\tilde{\mathbf{y}}_w = \tilde{\Omega}_{\hat{\theta}}\tilde{\mathbf{y}}_s^{\hat{\theta}}$, a necessary and sufficient condition is $P < \text{Spark}(\tilde{\Omega}_{\hat{\theta}})/2$. As a result, the maximum number of targets that can be detected is $M+N-2$.

Remark 5. In this paper, it is assumed that the targets can be considered to be precisely located at the discretized direction grid of the complete dictionary by reasonably setting the small cell size, i.e. they are on-grid. However, in realistic case, the targets may not lie in the dictionary, which is known as the off-grid problem [9,36]. Under this circumstance, the corresponding specific off-grid and gridless solutions have been proposed and thoroughly discussed in [29,37–39]. It can be concluded that based on the results of the proposed algorithm, off-grid sparse optimization methods including those based on a dynamic grid [37] or the joint estimation of the sparse signal and the grid offset [38], and gridless sparse methods such as those based on the atomic-norm minimization (ANM) [39], can be further used for reference to deal with the off-grid problem. In the field of the off-grid sparse DOA estimation, the application of the concept of the proposed reweighted smoothed l_0-norm minimization to the off-grid solutions, provides the prospect for reducing the computational complexity and improving the speed.

5. Simulation results

In this section, some simulations are performed to verify the effectiveness and the advantages of the proposed method. We compare the proposed method with the state-of-the-art l_1-SVD [9], reweighted l_1-SVD [18] and RV l_1-SRACV [20] algorithms. In addition, RD-Capon [8], RD-ESPRIT [7] and Cramér-Rao bound (CRB) [6] are also compared with the proposed method. The CRB is given by $\text{CRB}=\frac{\tau^2}{2J}\{\text{Re}[(\mathbf{D}^{\text{H}}\mathbf{\Pi}_A^{\perp}\mathbf{D}) \oplus \mathbf{R}_S^{\text{T}}]\}^{-1}$ [6,7,33,40], where $\oplus$ denotes the Hadamard product, τ^2 is the noise power, $\mathbf{\Pi}_A^{\perp} = \mathbf{I}_{MN} - \mathbf{A}(\mathbf{A}^{\text{H}}\mathbf{A})^{-1}\mathbf{A}^{\text{H}}$, and $\mathbf{D} = [\mathbf{d}_1, \mathbf{d}_2, \ldots, \mathbf{d}_P]$ with $\mathbf{d}_p = \partial[\mathbf{a}_t(\theta_p) \otimes \mathbf{a}_r(\theta_p)]/\partial\theta_p \in \mathbb{C}^{MN\times 1}$ being the 1st-order derivative of $\mathbf{a}_t(\theta_p)\otimes\mathbf{a}_r(\theta_p)$ with respect to θ_p, $p = 1, 2, \ldots, P$. The root mean square error (RMSE) of angle estimation is defined as $(1/P)\sum_{p=1}^{P}\sqrt{(1/Z)\sum_{i=1}^{Z}(\hat{\theta}_{p,i}-\theta_p)^2}$, where $\hat{\theta}_{p,i}$ is the estimator of the true target DOA θ_p for the ith Monte Carlo trial, Z is the total number of the Monte Carlo trials. In the simulations, $Z = 500$ is adopted. With half-wavelength $\lambda/2$ spaced ULAs, a narrowband monostatic MIMO radar system is considered. Therefore, the effective array aperture is $\bar{l}_a = (M+N-2)\lambda/2$. By collecting J snapshots, the received data matrix is obtained, which contains the Gaussian signals corresponding to the P uncorrelated targets and the Gaussian white noise. Meanwhile, the target number P is assumed to be known. The signal-to-noise ratio (SNR) is defined as $\text{SNR}=10\log_{10}(||\mathbf{AS}||_F^2/||\mathbf{N}||_F^2)$. Besides, the possible incident DOAs are considered from $-90°$ to $90°$, and this range is sliced to obtain the estimation grid. Considering $M = N = 5$ and $M = N = 7$ in the monostatic MIMO radar system, the Rayleigh resolution limit $\Delta\gamma = \frac{0.886}{\bar{l}_a/\lambda}$ is computed as $\Delta\gamma \approx 12.69°$ and $\Delta\gamma \approx 8.46°$, respectively. The cell size of the estimation grid in the complete dictionary is chosen as $0.05°$ for all of the analyzed sparse algorithms,

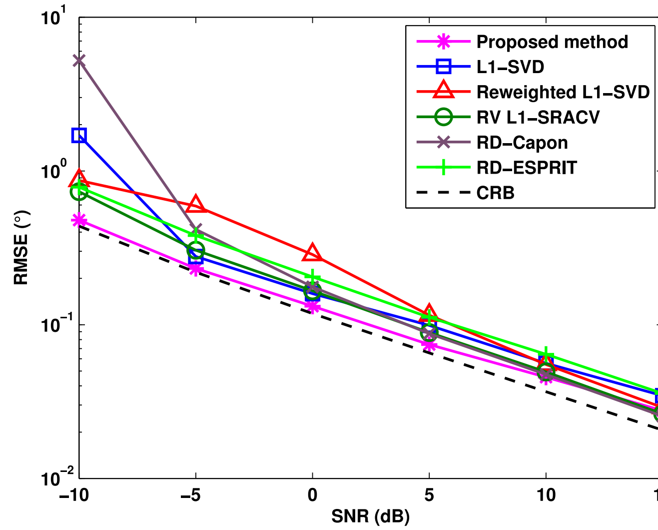

Fig. 1. RMSE versus SNR with three targets for $M = N = 5$.

so that $\mathbf{y}_s^{\hat{\theta}}$ is high-sparse and the targets can be assumed to be on-grid. The step size of RD-Capon is also $0.05°$. The parameters needed in the proposed method are set to $\sigma_1 = 4\max\{|\mathbf{v}_0|\}$, $Q = 3$ and $\mu = 2.5$. The decreasing factor $\alpha = 0.7$ is used to decrease σ gradually. Furthermore, we set $\sigma_{off} = 0.0004$ as the lower limit value of σ_K.

Fig. 1 depicts the RMSE of DOA estimation versus SNR for different methods, where $M = N = 5$, and the number of snapshots is $J = 600$. Additionally, three uncorrelated targets, whose DOAs are $\theta_1 = -12.8°$, $\theta_2 = 0°$ and $\theta_3 = 28.7°$, are considered. This simulation verifies that the RMSE of the proposed method is close to CRB. When SNR is below 10dB, the DOA estimation supplied by the proposed method has the least RMSE in all estimation results of the analyzed methods. In other words, the proposed method can provide better angle estimation performance than the other algorithms. This is because compared with the observation matrices $\mathbf{X}$ in Eq. (2) and $\bar{\mathbf{X}}$ in Eq. (7), the observation vector $\tilde{\mathbf{y}}_w$ of the proposed DOA estimation method enlarges the aperture of the corresponding virtual array. More specifically, the vector $\tilde{\mathbf{y}}_w$ is considered as the received data vector that corresponds to a virtual array and collects a single snapshot. For the pth target, the steering vector of the virtual array is $\mathbf{W}^{-\frac{1}{2}}[(\mathbf{Fb}(\theta_p)^*) \otimes (\mathbf{Fb}(\theta_p))]$, whose dimension is $(M+N-1)^2 \times 1$. The numbers of the unique elements in the steering vectors of $\mathbf{X}$, $\bar{\mathbf{X}}$ and $\tilde{\mathbf{y}}_w$, are $M+N-1$, $M+N-1$ and $2(M+N-1)-1$, respectively, which means that the proposed method enlarges the effective aperture to two times. Furthermore, in the proposed reweighted smoothed l_0-norm based sparse representation framework, the designed reweighted continuous function $f_\sigma(r_{wi}, y_{si}^{\hat{\theta}})$ and $F_\sigma(\mathbf{r}_w, \mathbf{y}_s^{\hat{\theta}})$ with the reweighted vector $\mathbf{r}_w$ reduces the impact of estimation errors of $\mathbf{R}_{\bar{X}}$ and enhances the smoothed solution of the l_0-norm.

Fig. 2(a) and (b) show the RMSE of DOA estimation in different methods versus angle separation, where $J = 600$, and SNR is fixed at SNR=0dB. In each method, there are two uncorrelated targets with DOAs being $\theta_1 = 0°$ and $\theta_2 = 0° + \Delta\theta$. The estimation results are evaluated with $\Delta\theta$ varying from $5°$ to $16°$. To compare the influence of different antenna numbers, $M = N = 5$ are used in Fig. 2(a), while $M = N = 7$ are used in Fig. 2(b). The comparison of Fig. 2(a) and Fig. 2(b) indicates that the performance of all analyzed methods is improved with the increase of the antenna numbers. Furthermore, it can be clearly seen from both Fig. 2(a) and (b) that for closely-spaced targets, the proposed method provides the

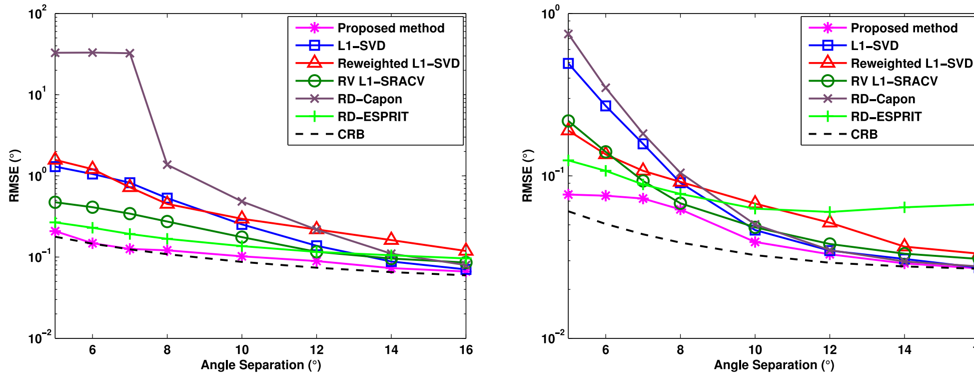

(a) $M = N = 5$ (b) $M = N = 7$

Fig. 2. RMSE versus angle separation with two targets.

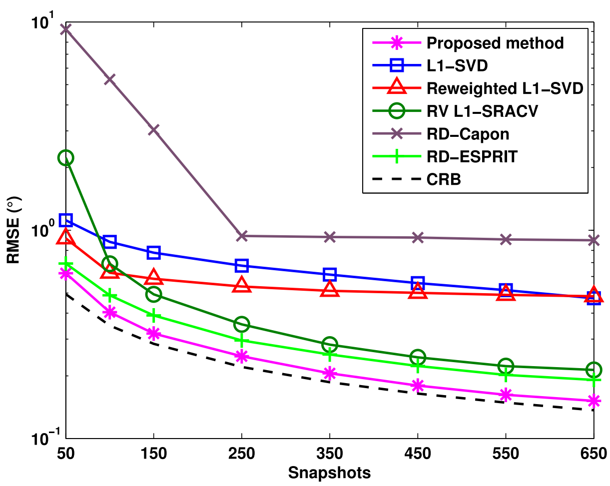

Fig. 3. RMSE versus snapshots with three targets for $M = N = 5$.

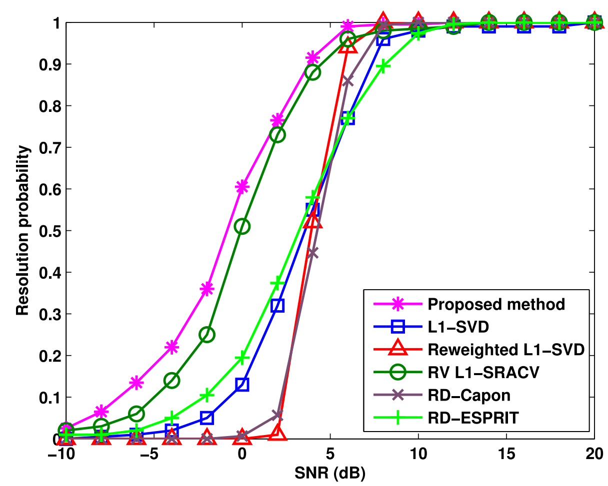

Fig. 4. Target resolution probability versus SNR with three targets for $M = N = 5$.

minimum RMSE. It means the proposed method can achieve higher spatial angular resolution than the other analyzed algorithms.

Fig. 3 demonstrates the RMSE of DOA estimation versus snapshots for different methods, with SNR fixed at SNR = 0dB. $M = N = 5$, and the number of the snapshots varies from $J = 50$ to $J = 650$. There are three uncorrelated targets located at $\theta_1 = -10^\circ$, $\theta_2 = 0^\circ$ and $\theta_3 = 10^\circ$, respectively. As can be seen from the figure, for all the methods, the estimation performance is improved with the increase of the snapshot number. In addition, the proposed method accomplishes the best DOA estimation in all snapshot region. Therefore, compared with the other analyzed algorithms, the proposed method has the better ability to adapt to low snapshots.

Fig. 4 illustrates the target resolution probability of different methods versus SNR, where $M = N = 5$, $J = 500$, and the DOAs of three uncorrelated targets are $\theta_1 = -11^\circ$, $\theta_2 = 0^\circ$ and $\theta_3 = 20^\circ$, respectively. In one trial, the targets are regarded as successfully detected when all of their absolute DOA estimation errors are within 0.1°. After all $Z = 500$ Monte Carlo trials, let $\hat{Z}_s$ denote the total number of the trials that successfully detect the three targets. Then the target resolution probability is defined as $\hat{Z}_s/Z$. In Fig. 4, when SNR is high enough, all methods can provide 100% target resolution probability. For each method, with the decrease of the SNR, the target resolution probability starts to drop at a certain point, which is defined as SNR threshold. It can be observed that the proposed method has the lowest SNR threshold, and it provides higher target resolution probability than all of the other analyzed algorithms.

Table 3 shows the computation time of these methods with different target numbers, where $M = N = 5$, $J = 500$ and SNR=0dB. For each method with P targets, the computation time is obtained from the average of $Z = 500$ trials. In each trial, with MATLAB software, the time is computed by the time in count (TIC) and time out count (TOC) instruction. Additionally, the DOAs of P uncorrelated targets $\{\theta_1, \theta_2, \ldots, \theta_P\}$ are generated by $\theta_p = (p-2)10^\circ$ with $p = 1, 2, \ldots, P$. As shown in Table 3, with more targets, the com-

Table 3
Average computation time of different DOA estimation algorithms.

P	Average Computation Time (s)					
	l_1-SVD	Reweighted l_1-SVD	RV l_1-SRACV	Proposed Method	RD-Capon	RD-ESPRIT
3	2.9536	3.1791	2.2165	0.0249	0.1834	0.0059
4	3.8975	4.1219	2.2718	0.0247	0.1904	0.0060
5	4.8863	5.1090	2.3108	0.0238	0.1960	0.0063

putation time of the l_1-SVD, reweighted l_1-SVD and RV l_1-SRACV methods increases, whereas the computation time of the proposed algorithm is comparable or even less. This is because when constructing the reweighted vector $\mathbf{r}_w$ with the noise subspace $\mathbf{U}_n \in \mathbb{C}^{(M+N-1)\times(M+N-1-P)}$, the dimension of $\mathbf{U}_n$ is reduced with the increase of the target number P, which results in the less calculation burden. Meanwhile, the computation time in Table 3 verifies that the proposed DOA estimation method is about two orders of magnitude faster than the l_1-SVD, reweighted l_1-SVD and RV l_1-SRACV algorithms. The proposed method has much lower computational complexity than the conventional l_1-norm minimization based DOA estimation methods.

6. Conclusion

In this paper, we have proposed a reweighted smoothed l_0-norm based DOA estimation algorithm for MIMO radar. In the proposed method, after the reduced dimensional transformation, the observation vector with a weighted matrix and the other reweighted vector are constructed. Then by solving the designed reweighted smoothed l_0-norm minimization framework, the DOAs of targets are obtained. The computational complexity has been analyzed, and the simulation results have verified that the computation time of the proposed method is about two orders of magnitude faster than that of the l_1-SVD, reweighted l_1-SVD and RV l_1-SRACV algorithms. Moreover, the proposed method provides better angle estimation performance and higher spatial resolution.

Acknowledgment

This work was supported by the China Scholarship Council and the Fundamental Research Funds for the Central Universities (HEUCF160401).

References

[1] E. Fishler, A. Haimovich, R. Blum, D. Chizhik, L. Cimini, R. Valenzuela, MIMO radar: an idea whose time has come, in: Proceedings of the IEEE Radar Conference, 2004, pp. 71–78. Philadelphia, PA, USA, 26–29 April.
[2] J. Li, P. Stoica, MIMO radar with colocated antennas, IEEE Signal Process. Mag. 24 (5) (2007) 106–114.
[3] W. Zhou, J. Liu, P. Zhu, et al., Noncircular sources-based sparse representation algorithm for direction of arrival estimation in MIMO radar with mutual coupling, Algorithms 9 (3) (2016) 61.
[4] W. Wang, X. Wang, et al., Conjugate ESPRIT for DOA estimation in monostatic MIMO radar, Signal Process 93 (7) (2013) 2070–2075.
[5] M. Viberg, B. Ottersten, T. Kailath, Detection and estimation in sensor arrays using weighted subspace fitting, IEEE Trans. Signal Process. 39 (11) (1991) 2436–2449.
[6] P. Stoica, A. Nehorai, MUSIC, maximum likelihood, and Cramer-Rao bound, IEEE Trans. Signal Process. 37 (5) (1989) 720–741.
[7] X. Zhang, D. Xu, Low-complexity ESPRIT-based DOA estimation for colocated MIMO radar using reduced-dimension transformation, Electron. Lett. 47 (4) (2011) 283–284.
[8] X. Zhang, Y. Huang, et al., Reduced-complexity Capon for direction of arrival estimation in a monostatic multiple-input multiple-output radar, IET Radar Sonar Navig. 8 (8) (2012) 796–801.
[9] D. Malioutov, M. Cetin, A.S. Willsky, A sparse signal reconstruction perspective for source localization with sensor arrays, IEEE Trans. Signal Process. 53 (8) (2005) 3010–3022.
[10] S. Chen, S.S. D. Donoho, M. Saunders, Atomic decomposition by basis pursuit, SIAM Rev. 43 (1) (2001) 129–159.
[11] J.A. Tropp, Greed is good: algorithmic results for sparse approximation, IEEE Trans. Inform. Theor. 50 (10) (2004) 2231–2242.
[12] I.F. Gorodnitsky, B.D. Rao, Sparse signal reconstruction from limited data using FOCUSS: a re-weighted minimum norm algorithm, IEEE Trans. Signal Process. 45 (3) (1997) 600–616.
[13] D.P. Wipf, B.D. Rao, Sparse bayesian learning for basis selection, IEEE Trans. Signal Process. 52 (8) (2004) 2153–2164.
[14] A. Chinatto, E. Soubies, et al., l_0-optimization for channel and DOA sparse estimation, International Workshop on Computational Advances in Multi-Sensor Adaptive Processing (CAMSAP), 13–16 Dec., 2015, doi:10.1109/CAMSAP.2015.7383797.
[15] I. Daubechies, M. Defrise, C. de Mol, An iterative thresholding algorithm for linear inverse problems with a sparsity constraint, Comm. Pure Appl. Math. 57 (2004) 1413–1457.
[16] Z. Liu, Z. Huang, Y. Zhou, Array signal processing via sparsity-inducing representation of the array covariance matrix, IEEE Trans. Aerosp. Electron. Syst. 49 (3) (2013) 1710–1724.
[17] J. Yin, T. Chen, Direction-of-arrival estimation using a sparse representation of array covariance vectors, IEEE Trans. Signal Process. 59 (9) (2011) 4489–4493.
[18] X. Wang, et al., A sparse representation scheme for angle estimation in monostatic MIMO radar, Signal Process. 104 (11) (2014) 258–263.
[19] J. Dai, et al., Direction-of-arrival estimation via real-valued sparse representation, IEEE Antennas Wirel. Propag. Lett. 12 (2013) 376–379.
[20] X. Wang, W. Wang, X. Li, J. Liu, Real-valued covariance vector sparsity-inducing DOA estimation for monostatic MIMO radar, Sensors 15 (11) (2015) 28271–28286.
[21] G.H. Mohimani, M. Babaie-Zadeh, C. Jutten, Complex-valued sparse representation based on smoothed l^0 norm, in: IEEE International Conference on Acoustics, Speech and Signal Processing, 2008, pp. 3881–3884.
[22] H. Mohimani, M. Babaie-Zadeh, C. Jutten, A fast approach for overcomplete sparse decomposition based on smoothed l^0 norm, IEEE Trans. Signal Process. 57 (1) (2009) 289–301.
[23] M.M. Hyder, K. Mahata, An improved smoothed l_0 approximation algorithm for sparse representation, IEEE Trans. Signal Process. 58 (4) (2010) 2194–2205.
[24] H. Mohimani, et al., Sparse recovery using smoothed l^0 (SL0): convergence analysis, Information Theory, cite as: arXiv:1001.5073v1.
[25] H. Bu, et al., Regularized smoothed l^0 norm algorithm and its application to CS-based radar imaging, Signal Process. 122 (5) (2016) 115–122.
[26] F.H. Juwono, Q. Guo, et al., Impulsive noise detection in PLC with smoothed L0-norm, in: IEEE International Conference on Acoustics, Speech and Signal Processing (ICASSP), 2015, pp. 3232–3236.
[27] H. Yan, J. Li, G. Liao, Multitarget identification and localization using bistatic MIMO radar systems, EURASIP J. Adv. Signal Process. (2008), doi:10.1155/2008/283483.
[28] S. Fortunati, R. Grasso, et al., Single snapshot DOA estimation using compressed sensing, in: 2014 IEEE International Conference on Acoustics, Speech and Signal Processing (ICASSP) 4–9 May, 2014, pp. 2297–2301, doi:10.1109/ICASSP.2014.6854009.
[29] Q. Bao, K. Han, et al., DLSLA 3-D SAR imaging algorithm for off-grid targets based on pseudo-polar formatting and atomic norm minimization, Sci. China-Inf. Sci. 59 (6) (2016), doi:10.1007/s11432-015-5477-5.
[30] G.H. Mohimani, M. Babaie-Zadeh, C. Jutten, Fast sparse representation based on smoothed l^0 norm, in: Proceedings of the 7th International Conference Independent Component Analysis and Signal Separation (ICA), 2007, pp. 389–396.
[31] B. Ottersten, P. Stoica, R. Roy, Covariance matching estimation techniques for array signal processing applications, Digital Signal Process. 8 (3) (1998) 185–210.
[32] M. Wax, T. Kailath, Detection of signals by information theoretic criteria, IEEE Trans. Acoust. Speech Signal Process. 33 (2) (1985) 387–392.
[33] J. Liu, X. Wang, W. Zhou, Covariance vector sparsity-aware DOA estimation for monostatic MIMO radar with unknown mutual coupling, Signal Process. 119 (2) (2016) 21–27.
[34] M.E. Davies, Y.C. Eldar, Rank awareness in joint sparse recovery, IEEE Trans. Inf. Theor. 58 (2) (2012) 1135–1146.
[35] J. Liu, W. Zhou, X. Wang, Fourth-order cumulants-based sparse representation approach for DOA estimation in MIMO radar with unknown mutual coupling, Signal Process. 128 (11) (2016) 123–130.
[36] S. Bernhardt, R. Boyer, S. Marcos, P. Larzabal, Compressed sensing with basis mismatch: performance bounds and sparse-based estimator, IEEE Trans. Signal Process. 64 (13) (2016) 3483–3494.
[37] J. Fang, F. Wang, et al., Super-resolution compressed sensing for line spectral estimation: an iterative reweighted approach, IEEE Trans. Signal Process. 64 (18) (2016) 4649–4662.
[38] Z. Yang, et al., Off-grid direction of arrival estimation using sparse bayesian inference, IEEE Trans. Signal Process. 61 (1) (2013) 38–43.
[39] Z. Yang, L. Xie, Enhancing sparsity and resolution via reweighted atomic norm minimization, IEEE Trans. Signal Process. 64 (4) (2016) 995–1006.
[40] A. Hassanien, S. Vorobyov, Transmit energy focusing for DOA estimation in MIMO radar with colocated antenna, IEEE Trans. Signal Process. 59 (6) (2011) 2669–2682.